Geothermics 72 (2018) 124–137

Contents lists available at ScienceDirect

Geothermics

journal homepage: www.elsevier.com/locate/geothermics

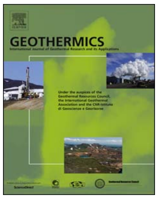

Failure mechanical behavior of pre-holed granite specimens after elevated temperature treatment by particle flow code

Sheng-Qi Yang*, Wen-Ling Tian, Yan-Hua Huang

State Key Laboratory for Geomechanics and Deep Underground Engineering, School of Mechanics and Civil Engineering, China University of Mining and Technology, Xuzhou, 221116, PR China

ARTICLE INFO

Keywords:
Pre-holed granite
High temperature
Cluster model
Mineral grain
Micro-crack
Measurement circle

ABSTRACT

Granite material, as an excellent medium for deep geological disposal rock projects may be affected by high temperature and macro-porosity. However, there are limited experiments and numerical simulations that have been adopted to investigate the failure mechanism of granite specimens that contain pre-existing holes after high temperature treatment. As such, the cluster model in PFC^{2D} was used to explore the *meso*-mechanics of granite specimens containing pre-existing holes with different ligament angles (the angle between the line connecting the centers of two holes and the horizontal direction, and set as $\beta = 0$, 45 and 90°) after different temperature treatments ($T = 25$, 150, 300, 450, 600, 750 and 900 °C). The different mineral grains in the granite specimen were simulated by the cluster model with different linear thermal expansion coefficients. The phase transition is treated as a radius expansion with 1.0046 of quartz cluster. The results show that the numerical simulation method is reasonable and the numerical results show good consistency with experimental results. The mechanical property curves can be divided into three phases, where the distribution of micro-cracks in a specimen has more scatter and fail more seriously with increasing temperature. The ligament angle has a significant effect on the crack evolution of a specimen. It was observed that more new micro-cracks with a scattered distribution existed in the high temperature treated specimen because the tensile force is concentrated at the temperature induced cracks. The ligament concentrates with compression in the H-model ($\beta = 0°$) specimen, and concentrates with shear stress in the D-model ($\beta = 45°$) specimen, while the ligament has almost no force concentration in the V-model ($\beta = 90°$) specimen. The first crack coalesced with holes as a shear crack regardless of the ligament angle, and the maximum values of shear stress decrease with increasing temperature.

1. Introduction

Deep geological disposal is an internationally accepted approach for the permanent disposal of high-level radioactive waste (HLW) (Zhao et al., 2016; Yang et al., 2017a). There has to be a systematic consideration of all thermal, hydrological and mechanical effects that could prejudice the integrity of the repository and its man-made and natural barriers in the short and long terms (Hudson et al., 2001; Yang et al., 2017b; Yang et al., 2017c; Zhou et al., 2015). Granite material is an excellent medium for deep geological disposal rock projects due to its lower permeability and better integrity (Yang et al., 2017a). As such, the time-dependent behavior (creep mechanical behavior) (Chen et al., 2017), strength and deformation properties (Shao et al., 2015), permeability (Chen et al., 2016), crack characteristics (Wang et al., 2015) and thermal conductivity (Zhao et al., 2016) of granite rocks at or after high temperature treatment has been investigated by many researchers (Homand-Etienne and Houpert, 1989; David et al., 1999; Chaki et al., 2008; Shao et al., 2014). Zhao et al. (2008) utilized Micro-CT to investigate granite under different temperatures. Yang et al. (2017a) used an X-ray micro CT scanning system and acoustic emission (AE) monitoring to investigate the internal crack and failure process of deformed granite specimens after different high temperatures. Kumari et al. (2017) investigated the stress-strain behavior under in situ stress and temperature conditions by conducting a series of high-pressure, high-temperature triaxial experiments. These experiments have greatly improved our understanding of thermal damage. Fan et al. (2017) conducted an experimental investigation of thermal effects on dynamic behavior of granite. Numerical modelling is also needed to investigate micro-mechanics behavior (Ghassemi, 2012). Zhao (2015) used the particle mechanics method to simulate the process of thermally induced micro- and macro-cracks in granite in order to elucidate the mechanisms responsible for temperature-dependent mechanical properties. Yu et al. (2015) adopted a mesostructured-based numerical model to analyse rock thermal cracking based on elastic damage mechanics and

---

* Corresponding author.
E-mail address: yangsqi@hotmail.com (S.-Q. Yang).

https://doi.org/10.1016/j.geothermics.2017.10.018
Received 16 June 2017; Received in revised form 22 September 2017; Accepted 23 October 2017

thermal-elastic theory.

It is well-known that porosity within rock masses and laboratory specimens influences the engineering properties of rock (Jespersen et al., 2010). Sammis and Ashby (1986) studied crack growth from a circular hole by loading plates of glass and of PMMA (Polymethyl Methacrylate) in compression. With the numerical code, MFPA^{2D} (Material Failure Process Analysis), Tang et al. (2005) studied the mechanisms of heterogeneous solids containing pre-existing single, tripe and multi-pore-like flaws under uniaxial compression. Wong et al. (2006) carried out a series of physical and numerical tests of uniaxial compression on sample containing a single hole with varied diameters and specimen widths to investigate the splitting failure, the failure modes and strength characterization. Wong and Lin (2015) used numerical simulation to investigate both crack initiation and crack coalescence mechanisms occurring in solids containing multiple holes under a state of uniaxial compression. Lin et al. (2015) examined crack initiation and coalescence mechanisms and failure behavior in a granite material containing multiple holes under uniaxial compression. Huang et al. (2017a) studied the strength behavior and crack evolution mechanism of granite containing pre-existing non-coplanar holes by experimental and numerical methods; four typical crack coalescence patterns were identified.

Macroporosity is familiar to the rock mechanics community because of the numerous characterization studies conducted at the proposed high-level nuclear waste repositories (Jespersen et al., 2010). However, limited laboratory experiments have been performed on the crack coalescence behavior of real rock specimens containing pre-existing holes after high temperature treatment (Huang et al., 2017b). Therefore, it is important to carry out research on the physical and mechanical behavior of granite containing macroporosity at or after elevated temperature treatment. Huang et al. (2017b) adopted an AE and photography monitoring technique to investigate crack initiation, propagation and coalescence behavior of pre-holed granite specimens after elevated temperature treatment. However, the *meso*-mechanics behavior of granite specimens containing pre-existing holes exposed to elevated temperatures has not been fully investigated. As such, the cluster model in two dimension particle flow code (PFC^{2D}) was used to simulate a crystalline granite specimen containing three holes with different ligament angle after different temperature treatments, in order to investigate crack number variation and crack evolution process. First, the applicability and reasonableness of the numerical simulation method was confirmed by comparison of stress-strain curves, peak strength, elastic modulus, peak strain and failure mode between experiments and numerical simulations. The crack evolution mechanisms of pre-holed granite specimens at room temperature and after 450 °C treatment were also analyzed by PFC^{2D}. Finally, the variation of stress with strain in the pre-holed specimens with different ligament angle after different high temperature treatments is discussed.

2. Numerical specimens and simulation procedure

Thermally induced strains are produced in the PFC^{2D} material by modifying the particle radius and the force carried in each parallel bond to account for heating of both particles and bonding material.

$$\Delta R = \alpha R \Delta T \tag{1}$$

$$\Delta F^n = -k^n A \Delta U^n = --k^n A(\bar{\alpha}\bar{L}\Delta T) \tag{2}$$

Where ΔR is particle radius change, α is the coefficient of linear thermal expansion, R is particle radius, ΔT is temperature increment; ΔF^n is the normal component of the force vector carried by the bond, K^n is the bond normal stiffness, A is the area of the bond cross section, $\bar{\alpha}$ is the expansion coefficient of the bond material and $\bar{L}$ is the bond length (Itasca Consulting Group, 2004).

Tested granite, taken from Quanzhou City in Fujian Province, China, has a crystalline and blocky structure, as shown in Fig. 1(a) (Huang et al., 2017b). According to the results of X-ray diffraction (XRD), the minerals components of the granite material are primarily Calcite (42.9%), Illite (11.4%), Biotite (23%) and Quartz (22.7%). Fig. 1(b) shows the numerical specimen generated by PFC^{2D} (Tian et al., 2017) and each numerical specimen contains 6008 clusters (grouped by 5 particles). Based on individual cluster identification code, 2656 clusters are defined as Calcite, 608 clusters are defined as Illite, 1381 clusters are defined as Biotite, and 1363 clusters are defined as Quartz. The coefficient of linear thermal expansion is set as $14.0 \times 10^{-6}\,\mathrm{K}^{-1}$ for Calcite, $9.13 \times 10^{-6}\,\mathrm{K}^{-1}$ for Illite, $3.0 \times 10^{-6}\,\mathrm{K}^{-1}$ for Biotite and $24.30 \times 10^{-6}\,\mathrm{K}^{-1}$ for Quartz (Fei, 1995).

2.1. Confirmation of the micro-parameters of granite

During the calibration process, micro-parameters were confirmed by the trial and error method. Table 1 lists the micro-parameters for the granite specimens in this research (Tian et al., 2017). The effective Young's modulus of the particle and parallel bond are both 25 GPa, and the ratio of normal to shear stiffness of the particle and the parallel bond are both 1.5. The values of the intra-cluster parallel-bond normal and shear strength are 180 ± 30 MPa and 280 ± 60 MPa, respectively. The values of the inter-cluster parallel-bond normal and shear strength are 90 ± 20 MPa and 140 ± 30 MPa, respectively.

After the calibration process, the specimens were heated. The temperature changed uniformly by 5 °C at every step and cycle of the model until the ratio of maximum unbalanced force divided by average force over all particles was equal or less to 0.01 (to minimize thermal shocks). The radius expansion of 1.0046 (Carpenter et al., 1998) is applied to the quartz cluster to simulate phase transition ($T = 573$ °C), and the quartz particle radius shrink with 0.9954 when the temperature decrease to 573 °C.

2.2. Calibrating micro-parameters by experimental results of granite at elevated temperature

Fig. 2 presents the comparison of stress-strain curves between experimentation and numerical simulation. From Fig. 2 it can be seen that the stress-strain curves of the granite specimen after different temperature show two different types, i.e., the brittle and ductile behaviors at the post-peak stage. The stress displays a suddenly drop after peak point, when T ≤ 450 °C. However, the stress drops slowly after peak point, when T ≥ 600 °C.

Fig. 3 illustrates the comparison between experimental and numerical peak strength, elastic modulus and peak axial strain of granite specimens after different temperatures. It is clear that the trend of peak strength, elastic modulus and peak strain with increasing temperature obtained by the numerical method is similar to those obtained by experimentation. Moreover, the numerical values are similarly equal to that obtained by experimentation at the same temperature. Like the experimental results, the mechanical property variation can be divided into three phases. Phase 1 (T ≤ 150 °C): the peak strength and peak strain are almost constant; Phase 2 (150 °C ≤ T ≤ 600 °C): the peak strength and elastic modulus decrease significantly, whereas peak strain increases; Phase 3 (600 °C ≤ T ≤ 900 °C): the peak strength and elastic modulus decrease gradually, while peak stain increases.

Fig. 4 shows the ultimate failure modes of intact granite specimens under compression after different high temperature treatments, as obtained by experimentation and numerical simulation (Huang et al., 2017b; Tian et al., 2017). The red and blue segment in specimens below 450 °C represent tensile and shear micro-crack, while the ultimate failure mode of specimens above 600 °C is presented by block with different colors (the block is separated by a crack, in order to illustrate the failure of specimens after higher temperature treatment). The failure modes of intact granite obtained by numerical simulation are approximate to those obtained by experimentation (Huang et al., 2017b). The distributions of micro-cracks in the specimen are more